J. Fac. Pharm. Ankara / Ankara Ecz. Fak. Derg., 47(3): 978-986, 2023
Doi: 10.33483/jfpau.1311496

ORIGINAL ARTICLE / ÖZGÜN MAKALE

IN SILICO EVALUATION OF SARS-COV-2 PAPAIN-LIKE PROTEASE INHIBITORY ACTIVITY OF SOME FDA-APPROVED DRUGS

FDA ONAYLI BAZI İLAÇLARIN SARS-COV-2 PAPAİN-LİKE PROTEAZ İNHİBİTÖR AKTİVİTESİNİN İN SİLİKO DEĞERLENDİRİLMESİ

Meryem EROL[1]*

[1]Erciyes University, Faculty of Pharmacy, Department of Pharmaceutical Chemistry, 38039, Kayseri, Turkey

ABSTRACT

Objective: *In this study, it was aimed to perform in silico studies on the papain-like protease structure of SARS-CoV-2 (PDB: 7JIT) of 1300 FDA-approved drugs downloaded from the ZINC database.*
Material and Method: *A molecular docking study was performed with PLpro (PDB ID: 7JIT) using four different molecular docking programs for a total of 1300 FDA-approved drugs obtained from the ZINC database. Conivaptan and amphotericin B were obtained in docking analysis with AutoDock Vina and Sybyl-X, respectively. Docking analysis with Glide SP and Glide XP resulted in fludarabine and panobinostat, respectively. Molecular dynamics simulations were performed for a period of 120 ns to check the stability of these four drugs.*
Result and Discussion: *The reliability of the results obtained using four different molecular docking programs on the SARS-CoV-2 papain-like protease of 1300 drug molecules was checked by reinserting the co-crystal ligand. Protein-ligand interactions between fludarabine, conivaptan, amphotericin-B, panobinostat, and PLpro were given. In the molecular dynamics study, RMSD, RMSF, Rg, and SASA analyses were performed for four systems. It was observed that RMSD remained constant for all 120 ns for all four systems except for amphotericin B, which deviated slightly towards the end of 120 ns. No significant fluctuation was noticed in the RMSF graphics for all four systems.*
Keywords: *Molecular docking, molecular dynamics, SARS-CoV-2, ZINC*

ÖZ

Amaç: *Bu çalışmada ZINC veri tabanından indirilen 1300 adet FDA onaylı ilacın SARS-CoV-2'nin papain-like proteaz yapısı üzerinde (PDB:7JIT) in siliko çalışmalarının yapılması amaçlanmıştır.*

* **Corresponding Author / Sorumlu Yazar:** Meryem Erol
e-mail / e-posta: eczacimeryem@gmail.com, **Phone / Tel.:** +903522076666-28350

Submitted / Gönderilme : 08.06.2023
Accepted / Kabul : 21.08.2023
Published / Yayınlanma : 20.09.2023

Gereç ve Yöntem: *ZINC veri tabanından elde edilen toplam 1300 FDA onaylı ilaç, dört ayrı moleküler doking programı kullanılarak PLpro (PDB ID: 7JIT) ile moleküler doking çalışması gerçekleştirildi. AutoDock Vina ve Sybyl-X ile doking analizinde, sırasıyla conivaptan ve amfoterisin B elde edildi. Glide SP ve Glide XP ile doking analizi sırasıyla fludarabin ve panobinostat ile sonuçlandı. Bu dört ilacın stabilitelerini kontrol etmek için 120 ns'lik bir süre boyunca moleküler dinamik simülasyonları gerçekleştirildi.*
Sonuç ve Tartışma: *1300 ilaç molekülünün SARS-CoV-2 papain benzeri proteazı üzerinde dört farklı moleküler doking programı kullanılarak elde edilen sonuçların güvenilirliği, ko-kristal ligandın yeniden yerleştirilmesiyle kontrol edildi. Fludarabin, conivaptan, amphotericin-B, panobinostat ve PLpro arasındaki protein-ligand etkileşimleri verildi. Moleküler dinamik çalışmasında dört sistem için RMSD, RMSF, Rg ve SASA analizleri yapıldı. 120 ns'nin sonlarına doğru hafifçe sapan amfoterisin B hariç, RMSD'nin dört sistemde de 120 ns'nin tamamında sabit kaldığı gözlendi. Dört sistemin tümü için RMSF grafiklerinde önemli bir dalgalanma fark edilmedi.*
Anahtar Kelimeler: *Moleküler dinamik, moleküler doking, SARS-CoV-2, ZINC*

INTRODUCTION

Coronaviruses (CoVs) are enveloped RNA viruses that have been responsible for three life-threatening viral epidemics in the last 20 years. They feature a 30 kb non-segmented positively sensitive RNA genome that has been known since the mid-1960s [1,2]. According to the World Health Organization, there were 8096 confirmed cases of SARS (severe acute respiratory syndrome) in 2002-2003 (mortality = 9.6%) and 2494 confirmed cases of MERS (Middle East respiratory disease) between 2012 and 2016. As of August 16, 2023, there were 769,774,646 confirmed COVID-19 cases, with 6,955,141 deaths reported to the WHO. The actual number is believed to be significantly higher. The invisible part of the iceberg brings along uncertainties. As a result, COVID-19 is the most serious epidemic to threaten humanity, both physically and financially, since the Spanish flu of 1918-1920. One of the most crucial areas being researched is the disease's spread patterns. The virus is known to spread in the foreground through droplets produced by coughing, sneezing, or talking. Fever, cough, shortness of breath, nasal discharge, nasal congestion, sneezing, sore throat, and smell and taste problems are the most prevalent symptoms. The binding of distinct cellular receptors and various structural characteristics of S-proteins explain these clinical symptom discrepancies. These variables all contributed to COVID-19's rapid dissemination [3,4].

The target cell membrane is bound by the S protein homotrimer, which creates projections on the virus surface. The virion is shaped by the M protein. The E protein is involved in virus recovery and release. The N protein is involved in virion packing and virus integrity versus intracellular defense mechanisms [5]. Although the roles of the majority of non-structural proteins (NSPs) in viral replication have been determined, the roles of a few remain unknown [6]. Viral proteases are an appealing target for therapeutic development since they are essential for viral replication. It is unique to each virus, allowing for targeted therapies with the minimum of hazardous side effects. Antagonizing ubiquitin and ubiquitin-like changes is a frequent strategy by which viral proteases influence innate immune pathways [7]. SARS-CoV-2 encodes two functioning proteases: papain-like protease (PLpro, NSP3) and 3-chymotrypsin-like cysteine protease (Mpro or 3CLpro, NSP5) [8]. PLpro produces NSP1, NSP2, and NSP3, and 3CLpro generates the remaining 13 non-structural proteins [7]. Mpro's primary job as a positive RNA virus is to degrade viral polyproteins that are required for virus development, replication, and invasion [9]. Inhibition of PLpro affects virus replication through inadequate viral protein processing and may also affect distant PLpro activities including deubiquitination, de-ISGylation, and innate anti-host immune reactions [10]. SARS-CoV PLpro is a cysteine protease with several major functions, including the processing of the viral polyprotein chain for viral protein maturation, irregular host inflammation responses by deubiquitylation, and disrupting host type I interferon antiviral immune responses by removing interferon-induced gene 15 [11]. Thus, inhibition of PLpro activity can halt viral replication and impair its role in host immune response evasion, making it an excellent anti-viral drug target.

In this study, a molecular docking study of 1300 FDA-approved drug molecules obtained from

the ZINC database (https://zinc.docking.org/) was performed on the crystal structure of Papain-Like Protease (PDB: 7JIT) of SARS CoV-2 using four separate programs. Molecular docking studies of all compounds were performed on AutoDock Vina, Glide SP, Glide XP, and Sybyl-X programs. The results of the studies were evaluated separately and a compound with the best binding energy (kcal/mol) was selected in each program. Conivaptan was obtained in docking analysis with AutoDock Vina, amphotericin B was obtained in docking analysis with Sybyl-X, fludarabine was obtained in docking analysis with Glide SP, and panobinostat was obtained in docking analysis with Glide XP (Figure 1). The reliability of all programs was checked by re-docking of the co-crystal ligand. The RMSD values and protein-ligand interactions of these drugs were given and presented with visuals. In addition, molecular dynamics simulations were performed using Gromacs Version 2020.4 for a period of 120 ns to check the stability of these four drugs. RMSD, RMSF, Rg, SASA values, and intermolecular hydrogen bond numbers for all systems were presented with graphics.

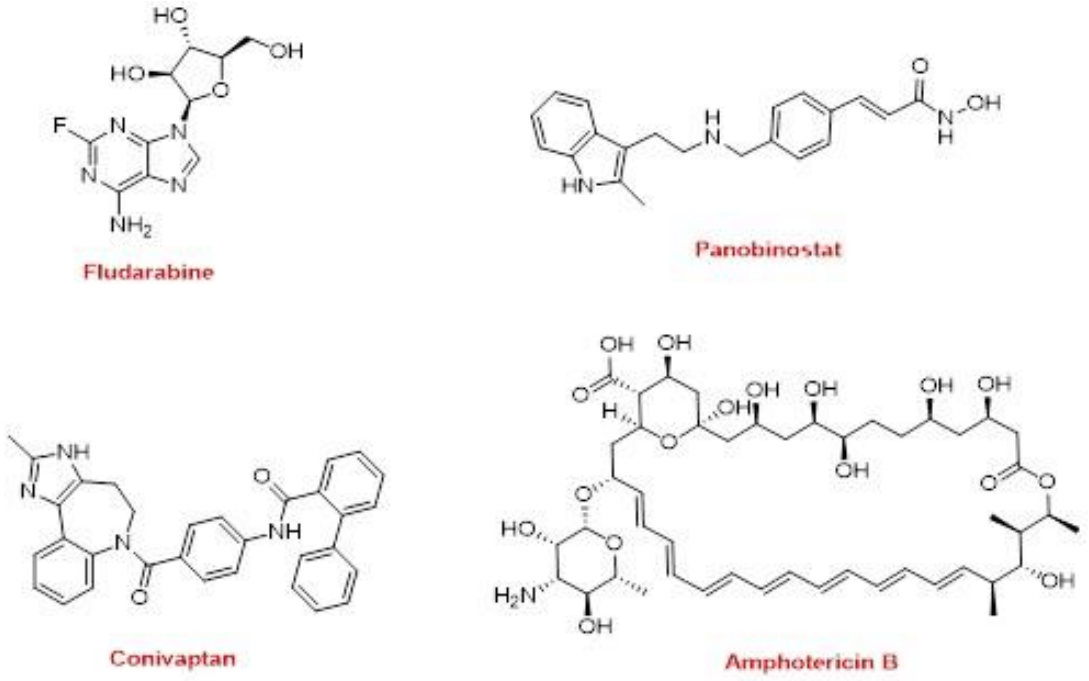

Figure 1. Chemical structures of fludarabine, panobinostat, conivaptan, and amphotericin-B

MATERIAL AND METHOD

Molecular Docking

Molecular docking studies were performed using Schrödinger Glide SP (Standard Precision) [12] and Glide XP (Extra Precision) [13], Autodock Vina v1.1.2 [14], and Sybyl-X v2.1.1 software [15]. The 3D crystal structure of the papain-like protease was downloaded from the protein databank (PDB:7JIT) [16]. Protein preparation was performed using the 'Protein Preparation Wizard' module of the Schrödinger suite (release 2022-3). 1300 FDA-approved drug molecules downloaded from the ZINC database [17,18] were downloaded in 3D SDF file format. The ligands were prepared using the 'LigPrep' module of the Schrödinger suite. The results of the studies performed in AutoDock Vina, Glide SP, Glide XP, and Sybyl-X programs were evaluated. 2D and 3D interactions of ligand and protein were determined and exhibited via BIOVIA Discovery Studio Visualizer v21.1 and UCSF Chimera v1.17.1.

Molecular Dynamics Simulation

Molecular dynamics simulations were performed using Gromacs Version 2020.4 [19]. The

procedure was carried out using the method given in the literature [20-22]. Root mean square deviation (RMSD) and root mean square fluctuation (RMSF), the radius of gyration (Rg), and solvent accessible surface area (SASA) analyses were performed in a standard molecular dynamics simulation of 120 ns duration. Molecular dynamics simulation trajectories were monitored with VMD-Visual Molecular Dynamics v1.9.4 and graphs were generated with the QtGrace Tool v0.2.6.

RESULT AND DISCUSSION

Molecular Docking

Traditional ways of discovering novel medicinal medications are costly and time-consuming. For this reason, many experimental and high-throughput simulation methods have been used in drug design in recent years. The "Molecular Docking Method" is one of these methods. Molecular docking studies are critical in identifying whether or not the millions of molecules thus produced are useful therapeutic ingredients. It is impossible to analyze each of the millions of chemical substances *in vitro*; thus, molecular docking studies play a critical role in determining the most effective molecules [23-25].

A total of 1300 FDA-approved drugs obtained from the ZINC database were subjected to molecular insertion with PLpro (PDB ID: 7JIT) using four molecular docking software programs. All programs were checked for their reliability by re-docking the co-crystal ligand, resulting in acceptable RMSD values of 1.002 Å (AutoDock Vina), 0.824 Å (Glide SP), 0.772 Å (Glide XP) and 0.826 (Sybyl-X) (Figure 2). After this validation, the docking of FDA-approved drugs was carried out using the same parameters for each software. Docking analysis with AutoDock Vina and Sybyl-X resulted in the acquisition of conivaptan and amphotericin B, respectively. Docking with the Glide program resulted in fludarabine and panobinostat from SP and XP docking, respectively. The four compounds acquired also showed molecular interactions with various residues of PLpro at the active site (Figure 3). In Table 1, protein-ligand interactions between fludarabine, conivaptan, amphotericin-B, panobinostat, and papain-like protease (PDB ID: 7JIT) were given. Molecular dynamics simulations were also performed to check the stability of these four drugs.

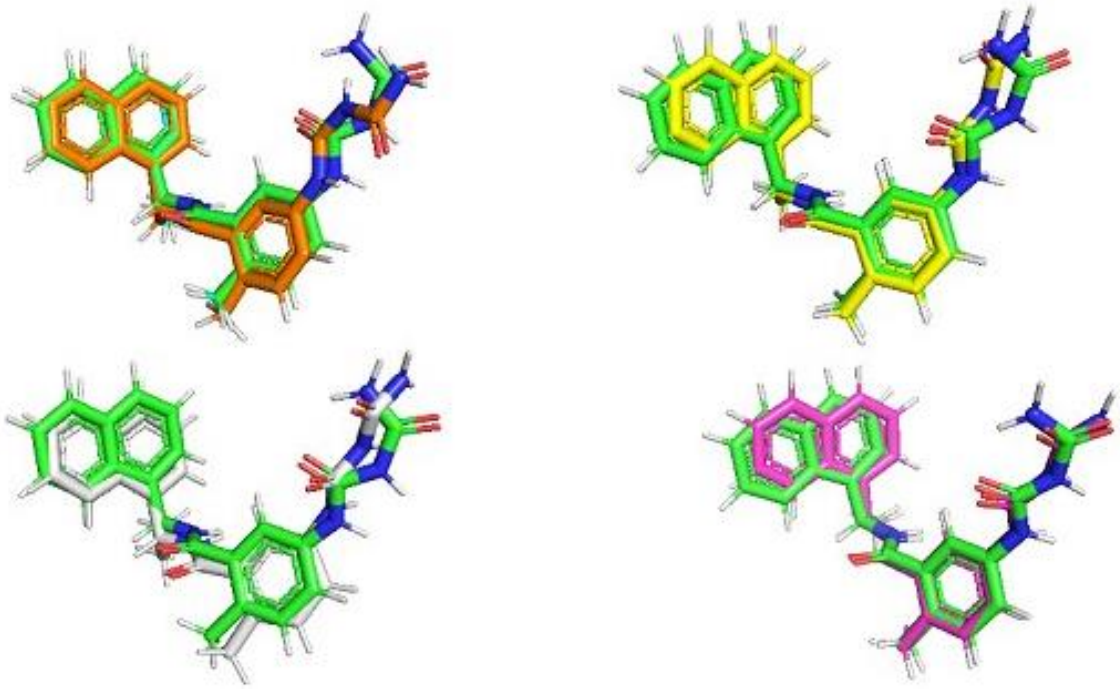

Figure 2. Superimposition of docking poses obtained with AutoDock Vina (orange), Glide SP (yellow), Glide XP (magenta), and Sybyl-X (gray) with the natural conformation of Y95. RMSD values were measured as 1.002 with AutoDock Vina, Glide SP 0.824, Glide XP 0.772, and Sybyl-X 0.826, respectively

Table 1. Protein-ligand interactions between fludarabine, conivaptan, amphotericin-B, panobinostat, and papain-like protease (PDB ID: 7JIT)

Compound	Protein-ligand Interactions
Fludarabine	LEU A:162, TYR A:268, GLN A:269, GLY A:163, ASP A:164, ARG A:166
Panobinostat	GLY A:163, GLY A:271, LEU A:162, GLN A:269, ASP A:164, MET A:208, GLUA:167, PRO A:247
Conivaptan	TYR A:263, PRO A:248, ASP A:164, TYR A:264, PRO A:247, TYR A:268, LYS A:157
Amphotericin B	ASP A:164, ARG A:166, GLU A:167, GLN A:269, LEU A:162, TYR A:263, TYR A:268, TYR A:264, PRO A:248

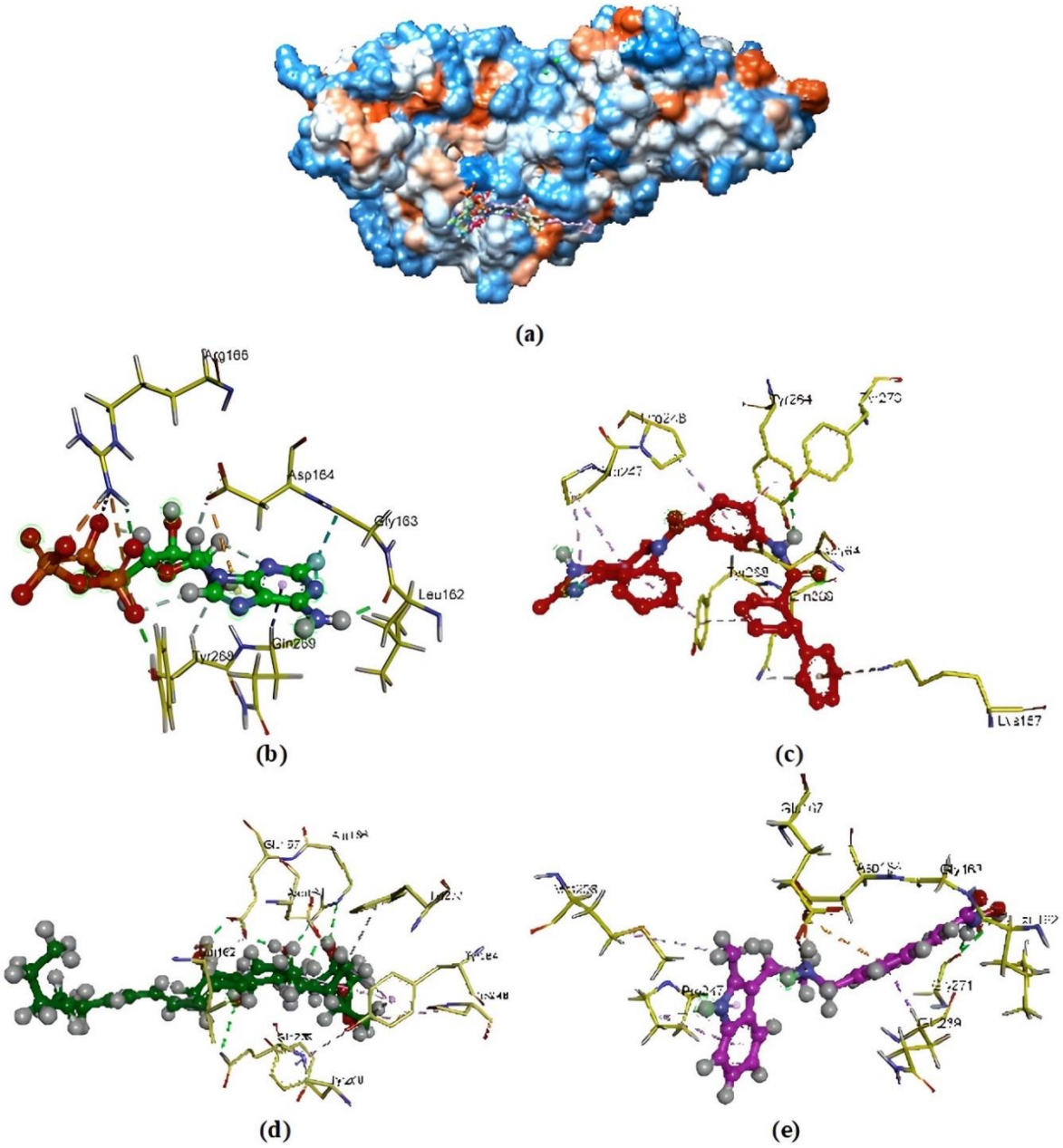

Figure 3. Protein-ligand interactions of superimposition (a), fludarabine (b), conivaptan (c), amphotericin B (d), and panobinostat (e) at the papain-like protease active site

Molecular Dynamics Simulations

Molecular dynamics (MD) simulations create an interface between experiment and theory by being used to predict the dynamic properties of complex systems that cannot be calculated analytically as the equivalent of experiments [26]. MD simulation systems are multi-particle systems that use numerical integration of Newton's Law of Motion's classical theory to describe the motion of atoms and molecules to construct a dynamic trajectory ranging from nanometer to micrometer scale. Such simulations help to answer significant unanswered questions in biology and chemistry. It also contributes continuously to the drug development process [27,28].

The docked complexes of the fludarabine, conivaptan, amphotericin-B, and panobinostat with PLpro were used as the beginning coordinates for molecular dynamics simulations, and their stabilities were tested for 120 ns. All systems were tested for stability by graphing their RMSD, RMSF, radius of gyration, and solvent-accessible surface areas (Figure 4).

The RMSD analysis indicates how much the atoms in the protein structure have shifted away from their normal positions before and during the simulations. RMSD analysis, in other words, enables the tracking of dynamic changes in protein structure. When an inhibitor is present in the active site of the target-containing residue in perfect protein-ligand MD simulations, it fluctuates less and interacts with the ligand [29]. The RMSD for all four systems was found to be steady for the whole 120 ns, with the exception of amphotericin B, which showed a minor departure near the end of the 120 ns.

The average deviation of a particle (for example, a protein residue) from a reference position (usually the particle's time-averaged position) over time is measured by RMSF [30]. As a result, the RMSF examines the parts of structures that deviate the most (or least) from their average structure.

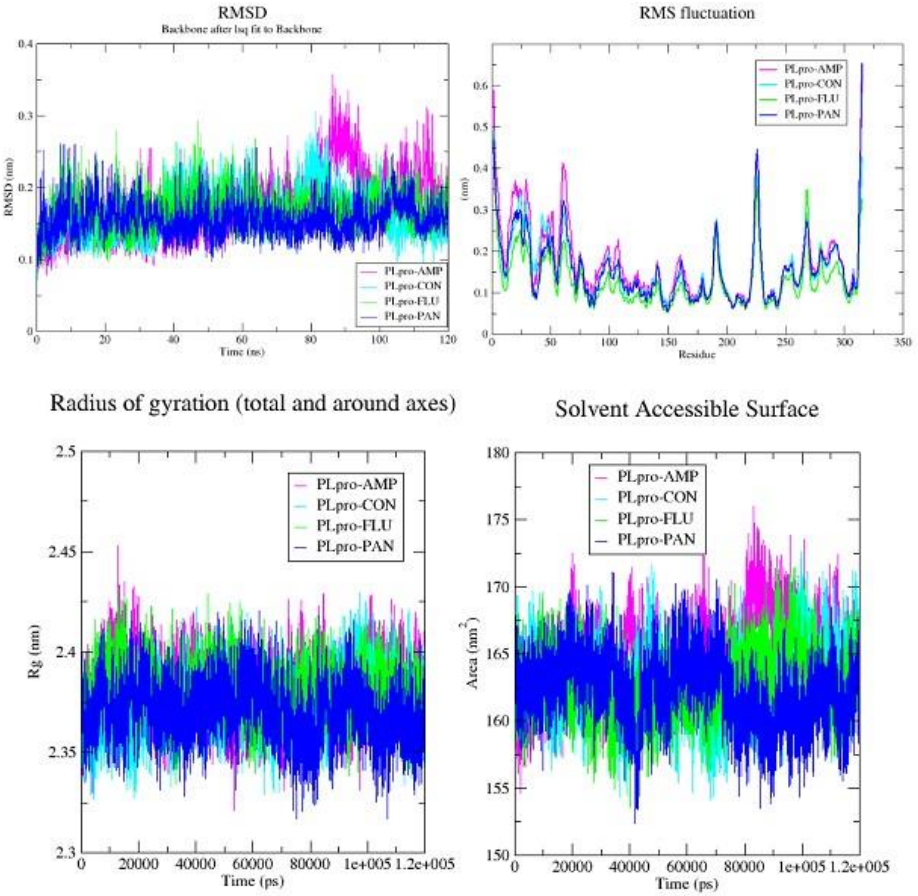

Figure 4. Molecular dynamics simulation of amphotericin B, conivaptan, fludarabine, and panobinostat with the papain-like protease active site. (a) RMSD of apo- and ligand-bound PLpro, (b) RMS fluctuation, (c) Rg, and (d) SASA values during the period of simulation

The Rg value, which is another analysis used to measure system stability, was also computed for each simulation group. A protein's radius of rotation (Rg) is a measure of its compactness. If a protein folds stably, its Rg value will most likely remain constant. If a protein unfolds rather than folding, its radius of rotation (Rg) changes over time [31]. As a result, the compactness of the four complexes was compared. It was measured with modest fluctuation values ranging from 2.32 to 2.45 nm. Over time, PLpro-CON, PLpro-FLU, and PLpro-PAN showed a more consistent trend.

The surface area of a biomolecular structure accessible by a solvent is defined as SASA (solvent accessible surface area) analysis [32]. To begin the modeling investigations, the SASA values of the four protein structures were determined and are shown in Figure 4. SASA measurements of fludarabine, conivaptan, amphotericin B, and panobinostat were done after binding to the active site of papain-like protease to determine the value of the solvent reaching the protein surfaces. The SASA value resulting from the interaction of amphotericin B with PLpro was larger than the others.

In protein-ligand or DNA-ligand interactions, the presence and amount of hydrogen bonds may signal that the ligand will interact more with the macromolecule and create a more stable complex [33]. As a result, the time-dependent number and fluctuation of hydrogen bonds were investigated. During the 120 ns simulation, as shown in Figure 5, amphotericin B typically has 1 to 4 hydrogen bonds, conivaptan has 1 to 5 hydrogen bonds, fludarabine has 1 to 8 hydrogen bonds, and panobinostat 1 to 7 hydrogen bonds.

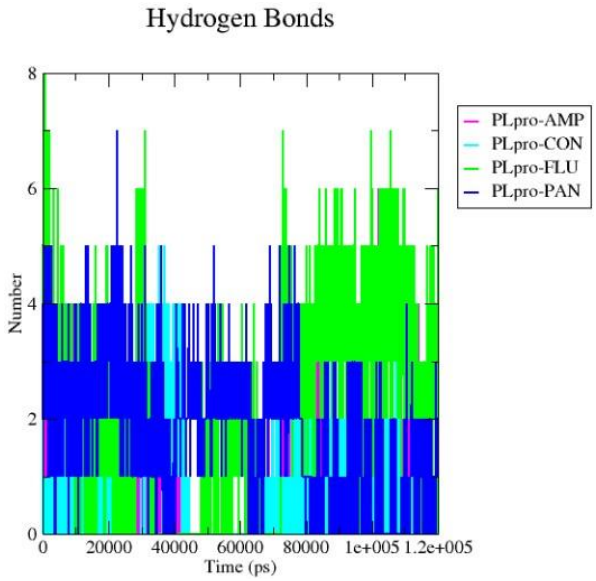

Figure 5. Intermolecular H bond number between papain-like protease active sites and amphotericin B, conivaptan, fludarabine, and panobinostat for 120 ns (PDB ID: 7JIT)

As a result, 1300 FDA-approved drugs collected from the ZINC database were molecular docked with PLpro (PDB ID: 7JIT) using four distinct molecular docking tools in this study. Protein-ligand interactions of drugs acquired by each program were demonstrated. In addition, molecular dynamics simulations were run for 120 ns to test the stability of these four drugs. All systems were subjected to RMSD, RMSF, Rg, and SASA evaluations, and all graphs were displayed. This study, which is supported by *in silico* research, will be valuable in identifying therapeutic compounds that are thought to be effective against SARS-CoV-2 PLpro.

ACKNOWLEDGEMENTS

All molecular dynamics simulations reported were performed utilizing TÜBİTAK (The Scientific and Technological Research Council of Turkey) ULAKBİM (Turkish Academic Network and Information Centre), High Performance and Grid Computing Centre (TRUBA resources).

AUTHOR CONTRIBUTIONS

Concept: M.E.; Design: M.E.; Control: M.E.; Sources: M.E.; Materials: M.E.; Data Collection and/or Processing: M.E.; Analysis and/or Interpretation: M.E.; Literature Review: M.E.; Manuscript Writing: M.E.; Critical Review: M.E.; Other: -

CONFLICT OF INTEREST

The author declares that there is no real, potential, or perceived conflict of interest for this article.

ETHICS COMMITTEE APPROVAL

The author declares that the ethics committee approval is not required for this study.

REFERENCES

1. Celik, I., Erol, M., Duzgun, Z. (2021). *In silico* evaluation of potential inhibitory activity of remdesivir, favipiravir, ribavirin and galidesivir active forms on SARS-CoV-2 RNA polymerase. Molecular Diversity, 26(1), 279-292. [CrossRef]
2. Rastogi, M., Pandey, N., Shukla, A., Singh, S.K. (2020). SARS coronavirus 2: from genome to infectome. Respiratory Research, 21, 1-15. [CrossRef]
3. Patel, K.P., Vunnam, S.R., Patel, P.A., Krill, K.L., Korbitz, P.M., Gallagher, J.P., Suh, J.E., Vunnam, R.R. (2020). Transmission of SARS-CoV-2: An update of current literature. European Journal of Clinical Microbiology and Infectious Diseases, 39, 2005-2011. [CrossRef]
4. Wang, Z., Fu, Y., Guo, Z., Li, J., Li, J., Cheng, H., Lu, B., Sun, Q. (2020). Transmission and prevention of SARS-CoV-2. Biochemical Society Transactions, 48(5), 2307-2316. [CrossRef]
5. Hasöksüz, M., Kilic, S., Sarac, F. (2020). Coronaviruses and Sars-CoV-2. Turkish Journal of Medical Sciences, 50(9), 549-556. [CrossRef]
6. Çelik, İ., Erol, M., Uzunhisarcikli, E., Ufuk, İ. (2022). Virtual screening and molecular docking analysis on three sars-cov-2 drug targets by multiple computational approach. Journal of Faculty of Pharmacy of Ankara University, 46(2), 376-392. [CrossRef]
7. Klemm, T., Ebert, G., Calleja, D.J., Allison, C.C., Richardson, L.W., Bernardini, J.P., Lu, B.G., Kuchel, N.W., Grohmann, C., Shibata, Y. (2020). Mechanism and inhibition of the papain-like protease, PLpro, of SARS-CoV-2. The EMBO Journal, 39(18), 1-17. [CrossRef]
8. Alamri, M.A., ul Qamar, M.T., Mirza, M.U., Alqahtani, S.M., Froeyen, M., Chen, L.L. (2020). Discovery of human coronaviruses pan-papain-like protease inhibitors using computational approaches. Journal of Pharmaceutical Analysis, 10(6), 546-559. [CrossRef]
9. Ullrich, S., Nitsche, C. (2020). The SARS-CoV-2 main protease as drug target. Bioorganic and Medicinal Chemistry Letters, 30(17), 127377. [CrossRef]
10. Gao, X., Qin, B., Chen, P., Zhu, K., Hou, P., Wojdyla, J.A., Wang, M., Cui, S. (2021). Crystal structure of SARS-CoV-2 papain-like protease. Acta Pharmaceutica Sinica B, 11(1), 237-245. [CrossRef]
11. Bosken, Y.K., Cholko, T., Lou, Y.C., Wu, K.P., Chang, C.A. (2020). Insights into dynamics of inhibitor and ubiquitin-like protein binding in SARS-CoV-2 papain-like protease. Frontiers in Molecular Biosciences, 7, 174. [CrossRef]
12. Friesner, R.A., Banks, J.L., Murphy, R.B., Halgren, T.A., Klicic, J.J., Mainz, D.T., Repasky, M.P., Knoll, E.H., Shelley, M., Perry, J.K. (2004). Glide: A new approach for rapid, accurate docking and scoring. 1. Method and assessment of docking accuracy. Journal of Medicinal Chemistry, 47(7), 1739-1749. [CrossRef]
13. Friesner, R.A., Murphy, R.B., Repasky, M.P., Frye, L.L., Greenwood, J.R., Halgren, T.A., Sanschagrin, P.C., Mainz, D.T. (2006). Extra precision glide: Docking and scoring incorporating a model of hydrophobic enclosure for protein-ligand complexes. Journal of Medicinal Chemistry, 49(21), 6177-6196. [CrossRef]
14. Trott, O., Olson, A.J. (2010). AutoDock Vina: Improving the speed and accuracy of docking with a new scoring function, efficient optimization, and multithreading. Journal of Computational Chemistry, 31(2), 455-461. [CrossRef]
15. Jain, A.N. (2007). Surflex-Dock 2.1: robust performance from ligand energetic modeling, ring flexibility, and knowledge-based search. Journal of Computer-aided Molecular Design, 21, 281-306. [CrossRef]
16. Osipiuk, J., Azizi, S.A., Dvorkin, S., Endres, M., Jedrzejczak, R., Jones, K.A., Kang, S., Kathayat, R.S., Kim, Y., Lisnyak, V.G. (2021). Structure of papain-like protease from SARS-CoV-2 and its complexes with non-covalent inhibitors. Nature Communications, 12, 1-9. [CrossRef]

17. Irwin, J.J. (2008). Using ZINC to acquire a virtual screening library. Current Protocols in Bioinformatics, 22(1), 14.6.1.-14.6.23. [CrossRef]
18. Irwin, J.J., Shoichet, B.K. (2005). ZINC-a free database of commercially available compounds for virtual screening. Journal of Chemical Information and Modeling, 45(1), 177-182. [CrossRef]
19. Abraham, M.J., Murtola, T., Schulz, R., Páll, S., Smith, J.C., Hess, B., Lindahl, E. (2015). GROMACS: High performance molecular simulations through multi-level parallelism from laptops to supercomputers. SoftwareX, 1, 19-25. [CrossRef]
20. Erol, M., Celik, I., Kuyucuklu, G. (2021). Synthesis, molecular docking, molecular dynamics, DFT and antimicrobial activity studies of 5-substituted-2-(*p*-methylphenyl)benzoxazole derivatives. Journal of Molecular Structure, 1234, 130151. [CrossRef]
21. Erol, M., Celik, I., Ince, U., Fatullayev, H., Uzunhisarcikli, E., Puskullu, M.O. (2022). Quantum mechanical, virtual screening, molecular docking, molecular dynamics, ADME and antimicrobial activity studies of some new indole-hydrazone derivatives as potent agents against E. faecalis. Journal of Biomolecular Structure and Dynamics, 40(17), 8112-8126. [CrossRef]
22. Erol, M., Celik, I., Sağlık, B.N., Karayel, A., Mellado, M., Mella, J. (2022). Synthesis, molecular modeling, 3D-QSAR and biological evaluation studies of new benzimidazole derivatives as potential MAO-A and MAO-B inhibitors. Journal of Molecular Structure, 1265, 133444. [CrossRef]
23. Fan, J., Fu A., Zhang, L. (2019). Progress in molecular docking. Quantitative Biology, 7, 83-89. [CrossRef]
24. Stanzione, F., Giangreco, I., Cole, J.C. (2021). Use of molecular docking computational tools in drug discovery. Progress in Medicinal Chemistry, 60, 273-343. [CrossRef]
25. Santos, L.H., Ferreira, R.S..Caffarena, E.R. (2019). Integrating molecular docking and molecular dynamics simulations. Docking Screens for Drug Discovery, Methods in Molecular Biology, 13-34. [CrossRef]
26. Eren, D., Yalçın, İ. (2020). Rasyonel ilaç tasarımında moleküler mekanik ve moleküler dinamik yöntemlerin kullanılma amacı. Journal of Faculty of Pharmacy of Ankara University. 44(2), 334-355. [CrossRef]
27. Salo-Ahen, O.M., Alanko, I., Bhadane, R., Bonvin, A.M., Honorato, R.V., Hossain, S., Juffer, A.H., Kabedev, A., Lahtela-Kakkonen, M., Larsen, A.S. (2020). Molecular dynamics simulations in drug discovery and pharmaceutical development. Processes, 9(1), 71. [CrossRef]
28. Durrant, J.D., McCammon, J.A. (2011). Molecular dynamics simulations and drug discovery. BMC Biology, 9(1), 1-9. [CrossRef]
29. Kirchmair, J., Markt, P., Distinto, S., Wolber, G., Langer, T. (2008). Evaluation of the performance of 3D virtual screening protocols: RMSD comparisons, enrichment assessments, and decoy selection-what can we learn from earlier mistakes? Journal of Computer-aided Molecular Design, 22, 213-228. [CrossRef]
30. Martínez, L. (2015). Automatic identification of mobile and rigid substructures in molecular dynamics simulations and fractional structural fluctuation analysis. PloS one, 10(3), e0119264. [CrossRef]
31. Ghahremanian, S., Rashidi, M.M., Raeisi, K., Toghraie, D. (2022). Molecular dynamics simulation approach for discovering potential inhibitors against SARS-CoV-2: A structural review. Journal of Molecular Liquids, 354, 118901. [CrossRef]
32. Boroujeni, M.B., Dastjerdeh, M.S., Shokrgozar, M., Rahimi, H., Omidinia, E. (2021). Computational driven molecular dynamics simulation of keratinocyte growth factor behavior at different pH conditions. Informatics in Medicine Unlocked, 23, 100514. [CrossRef]
33. da Fonseca, A.M., Caluaco, B.J., Madureira, J.M.C., Cabongo, S.Q., Gaieta, E.M., Djata, F., Colares, R.P., Neto, M.M., Fernandes, C.F.C., Marinho, G.S. (2023). Screening of potential inhibitors targeting the main protease structure of SARS-CoV-2 via molecular docking, and approach with molecular dynamics, RMSD, RMSF, H-bond, SASA and MMGBSA. Molecular Biotechnology, 1-15 (*in press*). [CrossRef]